How important is site conditions detailing and vulnerability modeling in seismic hazard and risk assessment at urban scale?

Kyriazis Pitilakis [1[0000-0003-2265-0314]], Evi Riga[1[0000-0001-5310-0505]] and Stefania Apostolaki[1[0000-0002-3377-0322]]

[1] Aristotle University of Thessaloniki, P.O.B. 424, 54124, Thessaloniki, Greece
kpitilak@civil.auth.gr

Abstract. This work investigates the effect of the level of detailing of site conditions as well as the selection of the fragility and vulnerability models on large scale seismic risk assessment. For this we consider the application of selected components of the recent European Seismic Hazard (ESHM20) and Risk (ESRM20) Models and we focus on Thessaloniki, Greece, a city which is very well documented in terms of local site conditions and exposure. Seismic risk results are compared in terms of expected damages and economic losses for a seismic hazard with a 475-year return period. The results indicate that the level of site conditions modelling does not significantly affect the estimated aggregate damages and economic losses at city scale, however significant discrepancies may occur at local scale. On the other hand, the selection of the vulnerability model for the building stock may considerably affect the intensity and the spatial distribution of damages, resulting in a considerable differentiation in the economic losses estimate.

Keywords: ESHM20, ESRM20, site modelling, site amplification, fragility and vulnerability models, seismic risk model

1 Introduction

In large-scale seismic hazard and risk studies the level of detailing of site conditions is a real challenge both from scientific and practical point. Site amplification of seismic ground motion due to the local site conditions and other induced phenomena, like liquefaction, may affect considerably the seismic hazard and the final risk assessment in terms of physical, human and immaterial losses. Regarding seismic hazard assessment at urban scale, and in the absence of detailed microzonation studies, which is a very common situation, site effects are necessarily estimated using simple parameters like $V_{s,30}$, i.e., the time-averaged shear wave velocity in the upper 30 meters of the soil deposits. Again, in large scale applications, $V_{s,30}$ values are often inferred from proxies such as the topographic slope and geology, or from simplified site categorization based on seismic codes site characterization and mapping. The risk assessment, on the other hand, for a given large scale urban building exposure, is conducted using fragility and

vulnerability models, which, due to the complexity and diversification of the building typologies, are usually of generic nature, while they are also tightly related to the intensity measures used, which in turn, are explicitly related to the results of the seismic hazard. It is evident that the uncertainties involved in all stages of this complex process are important and may affect the final risk assessment, with consequent high impact on the frame of strategic decision making.

To this regard, the scope of this work is to investigate on one hand the effects of the method applied for site characterization in the seismic hazard assessment and on the other hand the appropriateness of the selection of the vulnerability functions in urban large scale seismic risk assessment. For this we consider the application of selected components of the recent European Seismic Hazard (ESHM20, Danciu et al., 2021) and Risk (ESRM20, Crowley et al. 2021) Models and we focus on Thessaloniki, Greece, a city which is very well documented in terms of local site conditions, exposure and vulnerability curves specific for the main building typologies. Thessaloniki, located in Northern Greece, is the second largest city in Greece, with over 1 million inhabitants in its metropolitan area. The area studied herein, includes 16 municipalities and covers an area of 126 km^2 (Fig. 1).

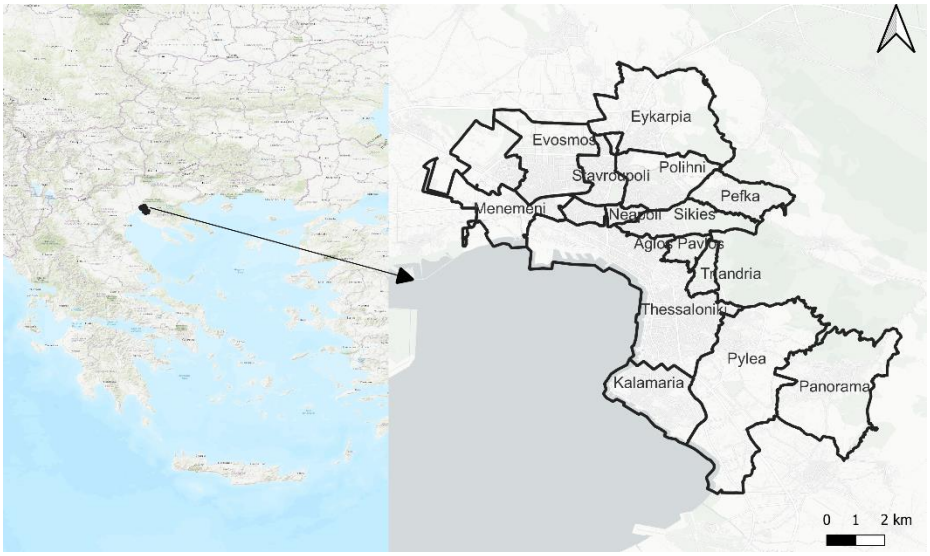

Fig. 1. Study area of Thessaloniki

To investigate the impact of the method applied for site modelling in seismic hazard assessment and of the selection of the vulnerability functions on the seismic risk assessment of Thessaloniki, we compare seismic risk results obtained using two different approaches for site conditions modelling for the seismic hazard combined with two different fragility and vulnerability models. Regarding site modelling for seismic hazard assessment, in the first approach, which may be considered as more rigorous but also more demanding, appropriate site models in terms of $V_{s,30}$ are directly used in the ESHM20 hazard logic tree, while in the second approach, which is more simplified and

efficient in practice, the study area is classified into different site classes based on a code-oriented classification scheme (Riga et al., 2022). With respect to fragility and vulnerability modelling, we apply two sets of analytical generic fragility and vulnerability models, recommended for large scale applications, i.e., the ESRM20 models (Romão et al., 2021), derived from equivalent single degree-of-freedom oscillators and the models by Kappos et al. (2006; 2010), derived from 2D numerical models of structures representative for Greece and Southern Europe in general.

Seismic risk results are presented in terms of expected damages and economic losses for a seismic hazard with a 475-year return period. Both hazard and risk assessment calculations are undertaken with the OpenQuake Engine (Pagani et al., 2014; Silva et al., 2014).

2 Site modelling and seismic hazard assessment

Thessaloniki is one of the best-documented urban areas in terms of local site conditions. In the framework of its microzonation study (Anastasiadis et al., 2001), a significant amount of laboratory and in situ geophysical and geotechnical surveys have been performed to validate the dynamic properties and geometry of the main soil formations and develop detailed geotechnical maps, 1-D profiles and 2-D cross sections.

In the present work, following Riga et al. (2022), we applied two different approaches for site modelling to assess the seismic hazard in the study area. In the first approach (Approach 1), we adopted a detailed site model developed for Thessaloniki using the available data from the microzonation study. The $V_{s,30}$ values of this model are shown in Fig. 2 for a grid consisting of 142 points, with a horizontal and vertical spacing of 0.01 geographic degrees (approximately 1x1 km). Based on this detailed site model, the north-east part of the city is situated on rock-like formations, with $V_{s,30}$ values greater than 800 m/s, and is therefore classified as soil type A according to EC8. $V_{s,30}$ at the coastal area ranges between 180 m/s and 360 m/s (EC8 soil class C/S2), while the in-between region consists of deposits with $V_{s,30}$ values between 360 and 800 m/s, and is categorized as EC8 soil type B (Fig. 2). In Approach 1 the $V_{s,30}$ values of Fig. 2 were directly used as input in the ESHM20 ground motion model (Kotha et al., 2020) to estimate with a classical probabilistic analysis the seismic hazard with a 475-year return period for the specific soil and site conditions of Thessaloniki. Median values of PGA and spectral accelerations, S_a, at 0.3s, 0.6s and 1.0s obtained with Approach 1 were stored for all grid points. The specific ground motion parameters were selected, as they are needed as intensity measures by the applied fragility and vulnerability models, as described in detail in Section 4. Although Approach 1 is a very rigorous method, it is also very demanding, as it entails the existence of a site model for the whole study area as well as advanced knowledge and skills on seismic hazard assessment by the user (Riga et al., 2022).

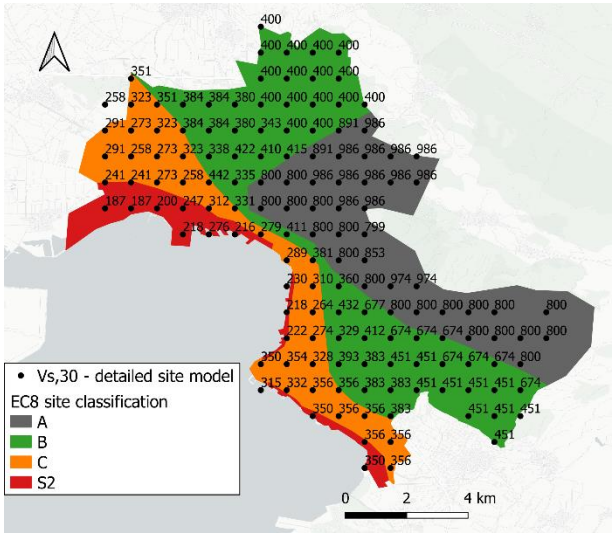

Fig. 2. Spatial distribution of $V_{s,30}$ (m/s) in the study area on the detailed site model developed from the microzonation study of Thessaloniki, applied in Approach 1 for seismic hazard assessment. The classification of the study area according to EC8 (CEN, 2004) based on the detailed site model is also included in the figure.

In the second Approach (Approach 2), we used the detailed site model to classify the study area into appropriate site classes following the classification scheme by Pitilakis et al. (2020), which uses as classification parameters the approximate depth to seismic bedrock, the equivalent shear wave velocity $V_{s,H}$ (equal to $V_{s,30}$ for soil deposits with depth greater than 30 m, otherwise equal to the mean shear wave velocity up to the seismic bedrock depth) and the fundamental period of the site T_0. The classification of the study area based on the Pitilakis et al. (2020) scheme is shown in Figure Fig. 3. Compared to the EC8 classification shown in Fig. 2, the Pitilakis et al. (2020) classification differs mainly in the coastal area, as it includes more site classes, and in the spatial extent of zones (B1: shallow very stiff soil deposits and B2: Intermediate depth stiff soil deposits whose mechanical properties increase with depth) and C (C1: deep stiff soil deposits and C3: deep soil deposits of medium stiffness) due to the difference in the definitions of the respective soil classes in the two site classification schemes. For the application of Approach 2 for seismic hazard assessment, we evaluated for the soil classes of Fig. 3 the period-dependent site amplification factors according to Pitilakis et al. (2020) as the ratio between the elastic response spectrum for each soil class and the elastic response spectrum soil class A which represents rock or rock-like site conditions. We should highlight that the amplification factors by Pitilakis et al. (2020) are intensity-dependent, i.e., they decrease for increasing levels of ground shaking, taking in this way soil nonlinearity into account. The resulting amplification factors for PGA and Sa at 1.0s, Sa(1.0s) are shown in Fig. 4. We observe that for the specific ground shaking levels, the amplification factors for Sa(1.0s) at the part of the coastal area classified as class D (deep soil deposits consisting of soft to medium stiffness clays

and/or loose sandy to sandy-silt formations with substantial fines percentage) - X (special soils requiring site-specific evaluations), and in Kalamaria region (see Fig. 1), classified as soil class C3 (deep soil deposits, consisting of medium dense sand and gravel and/or medium stiffness clay), the amplification factors for Sa(1.0s) range between 2.1 and 2.9, and are significantly higher than the respective factors for PGA, as well as the amplification factors of EC8 (Riga et al., 2022).

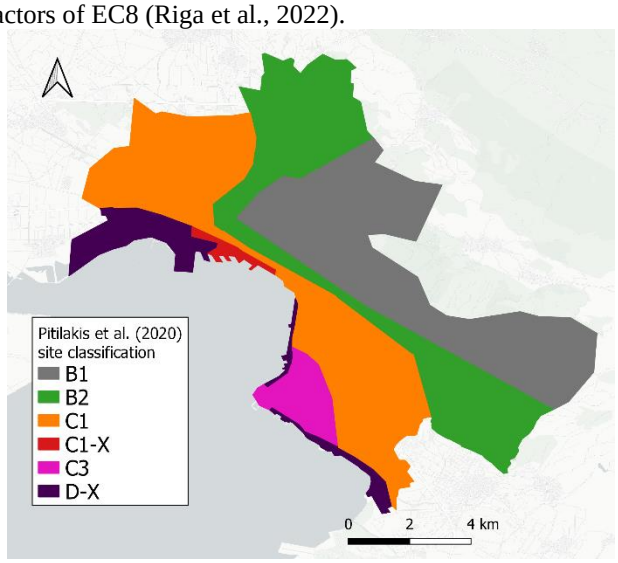

Fig. 3. Site classification of the study area based on the classification scheme by Pitilakis et al. (2020), applied in Approach 2 for seismic hazard assessment.

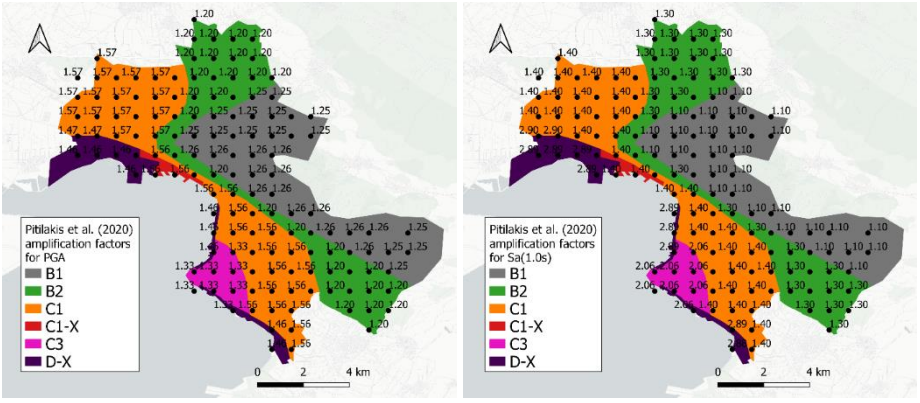

(a) (b)

Fig. 4. Spatial variability of the amplification factors in the study area according to Pitilakis et al. (2020) for mean return period of 475 years and for (a) PGA and (b) S_a(1.0s).

The amplification factors estimated for PGA and spectral accelerations, S_a, at 0.3s, 0.6s and 1.0s were then multiplied with the respective median ESHM20 hazard output for rock site conditions with a 475-year return period, publicly available through the hazard

platform of EFEHR (http://hazard.efehr.org). Compared to Approach 1, Approach 2 is more simplified and easier to be applied, as it entails a site classification of the study area based on a commonly applied site classification scheme and the existence of a seismic hazard assessment for rock-site conditions for the study area, both of which can be quite easily obtained (Riga et al., 2022).

Median values of PGA and spectral accelerations, S_a, at 0.3s, 0.6s and 1.0s obtained with both approaches were stored for all grid points. The spatial distribution of PGA and S_a(0.1s) at the ground surface obtained with Approaches 1 and 2 is compared in Fig. 5 and Fig. 6 respectively. Regarding PGA, the more detailed Approach 1 results in PGA values ranging between 0.27g at the rock-like formation and 0.45g at the coastal area, significantly higher than the respective PGA values obtained with Approach 2, where a maximum PGA equal to 0.38g is observed (Fig. 5). This trend is reversed for S_a(1.0s) is some areas(Fig. 6), especially at the part of the coastal area classified as soil class D-X, and in Kalamaria region, classified as soil class C3, where the Pitilakis et al. (2020) amplification factors for S_a(1.0s) are quite high (between 2.1 and 2.9), resulting in an overestimation of S_a(1.0s) with Approach 2 compared to Approach 1. This is expected to have a significant impact on the estimated damages at these regions, since one of the two adopted vulnerability models uses S_a(1.0s) as intensity measure for a significant number of buildings.

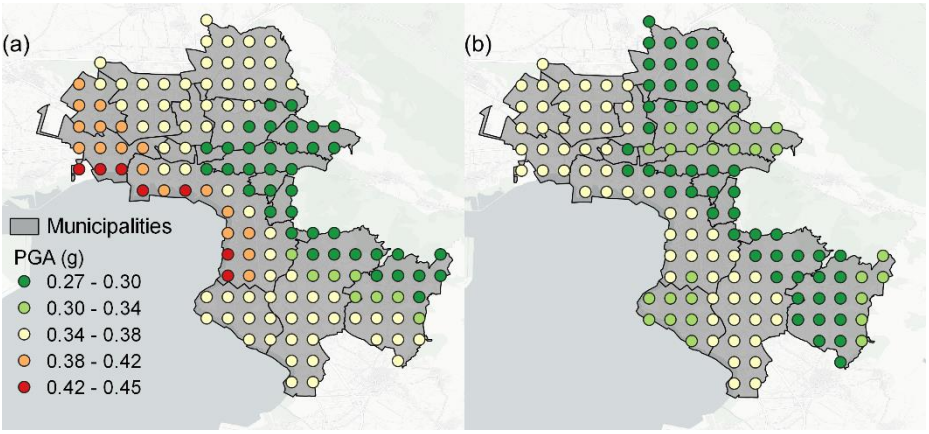

Fig. 5. Spatial distribution of PGA at the ground surface for seismic hazard with a 475-year return period obtained with (a) Approach 1 (detailed site model) and (b) Approach 2 (Pitilakis et al., 2020 classification system).

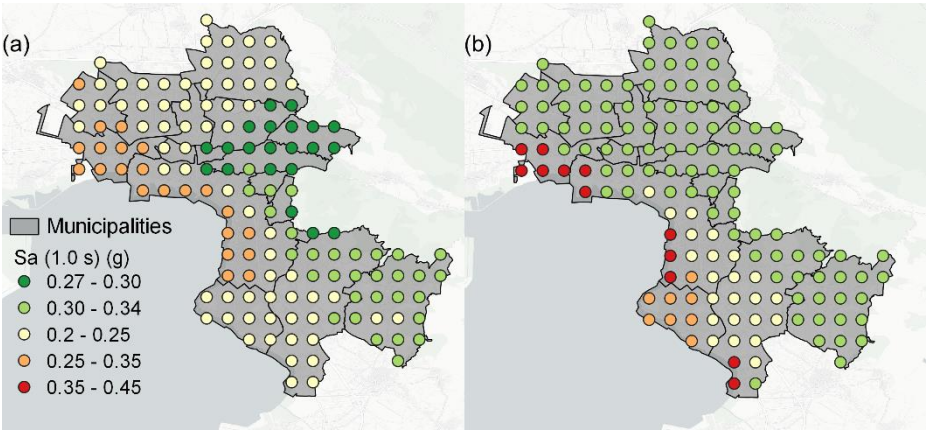

Fig. 6. Spatial distribution of S_a(1.0 s) at the ground surface for seismic hazard with a 475-year return period obtained with (a) Approach 1 (detailed site model) and (b) Approach 2 (Pitilakis et al., 2020 classification system).

3 Exposure model

For the development of the exposure model for the study area we used the data from the 2011 Population – Housing and Building Census (ELSTAT, 2011). The exposure model contains the residential buildings of the study area which are constructed either from reinforced concrete or masonry, as they constitute the vast majority of the residential buildings (99.7%) in the study area. The exposure model therefore contains 75,169 residential buildings that are either concrete, or unreinforced masonry (brick or stone).

These buildings were classified into different building classes following two different taxonomy schemes, the GED4ALL Building Taxonomy (Brzev et al., 2021), which is a uniform classification system developed by the Global Earthquake Model (GEM) aiming to be applicable at a global scale and is adopted in ESRM20 and the Kappos et al. (2006) classification scheme, specifically developed to address the Greek building stock. Both classification schemes use as classification attributes the main construction material, the lateral load resisting system, the height and the ductility level, which is herein assumed to be a function of the construction period and, thus, respective seismic design code in force at the time of the seismic event. The main differences of the two taxonomy schemes lie in the way the building height is defined in the different typologies and in the consideration or not of the soft-storeys, as described in detail in the following sections. Detailed data for the type of use, main construction material, number of storeys and the period of construction of the buildings are provided by the Hellenic Statistical Authority ELSTAT (2011) for each census sector of Thessaloniki. The census sector is the geographic unit adopted by ELSTAT for the census and contains an average of 600 residences. The lack of data for the lateral load resisting system has led to unavoidable assumptions based on the feedback from the SERA European

Building Exposure Workshop questionnaire (https://sites.google.com/eucentre.it/sera-exposure-workshop/questionnaire).

3.1 Exposure model following the GED4ALL Building Taxonomy scheme

Using the GED4ALL Building Taxonomy (Brzev et al., 2021), the residential buildings of the study area were classified according to the main construction material, the lateral load resisting system, the number of storeys (i.e. height), the ductility level, which is herein assumed to be a function of the construction period and, thus, respective seismic design code in force at the time of the seismic event, and lateral load coefficient used at the time of the design. The symbolization of each attribute is provided in Table 1. Level 1 is the first level of detail required to describe an attribute, whereas Level 2 provides additional detail on the Level 1 attributes. Building height is defined in terms of exact number of storeys. The existence of irregularly infilled frames with soft storey, which is a common practice in Greece, is not taken into account in this scheme, which is aimed to be applicable at a global scale.

The 75,169 residential buildings of the exposure model were finally classified in 107 building typologies. The vast majority (94.98%) of them are reinforce concrete (CR), while 59.7% have been designed with low level (DUCL or CDL) or even no seismic code (DNO or CDN). Fig. 7 shows the distribution of the examined residential buildings based on (a) the main construction material and lateral load resisting system, (b) the seismic code level and (c) the height expressed in terms of number of storeys.

Table 1. Values of attributes of GED4ALL Building Taxonomy (Brzev et al., 2021) used to describe the building stock of Thessaloniki.

Attribute	Element Code	Level 1 Value	Element Code	Level 2 Value
Material	CR	Concrete, reinforced		
	MUR	Masonry, unreinforced	CL99	Fired clay unit, unknown type
			STDRE	Stone
Lateral load-resisting system (LLRS)	LFM	Moment frame		
	LFINF	Infilled frame		
	LWAL	Walls and frames where the walls, due to their substantial lengths, resist the vast majority of the lateral load		
	LDUAL	Moment frames and shear walls acting together to resist seismic effects		
Ductility Level – Seismic Code Level	DNO or CDN	Non-ductile (Period of construction: before 1959)		
	DUCL or CDL	Ductile, low (Period of construction: 1960-1985)		
	DUCM or CDM	Ductile, medium (Period of construction: 1986-1995)		

	DUCH or CDH	Ductile, high (Period of construction: 1996-present)
Height	H	Exact number of storeys above ground
Lateral Force Coefficient	Number expressed in %	The value of the lateral force coefficient, i.e. the fraction of the weight that was specified as the design lateral force in the seismic design code (Applied to reinforced concrete moment and infilled frames only)

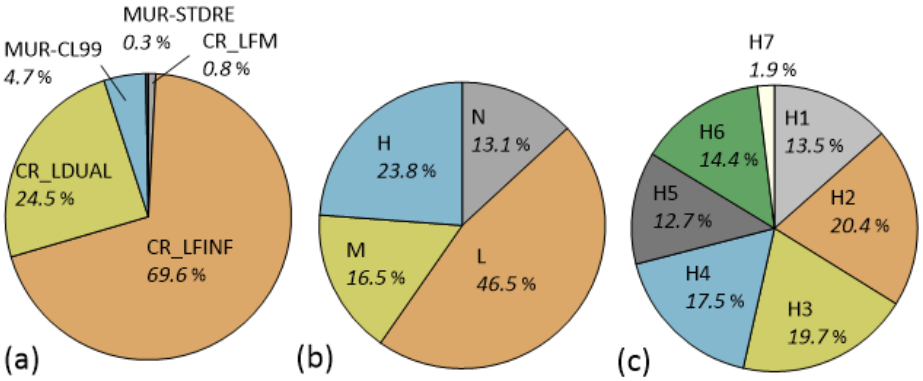

Fig. 7. Classification of the building taxonomies in the study area based on a) material and lateral load resisting system (LLRS), b) code level and c) height according to the GED4ALL Building Taxonomy scheme of Table 1.

3.2 Exposure model according to Kappos et al. (2006)

Using the taxonomy scheme defined by Kappos et al. (2006), which has been specifically developed to address the Greek building stock, the residential buildings of the study area were classified according to the main construction material, the lateral load resisting system, the height category, and the relevant seismic code level which is linked with the period of construction. The symbolization of each attribute is provided in Table 2. Regarding building height, this scheme provides three height categories defined in terms of ranges of number of storeys, while the existence of a soft storey (commonly referred to as pilotis in Greece) is considered.

The 75,169 residential buildings of the exposure model were classified in 64 building typologies. Most of the buildings (75.6%) are regularly infilled reinforced concrete buildings (CR) whereas 18.45 % are irregularly reinforced as they have at least one soft-storey. Fig. 8 shows the distribution of these buildings based on (a) the main construction material and lateral load resisting system, (b) the seismic code level and (c) the height category.

Table 2. Values of attributes of Kappos et al. (2006) taxonomy scheme used to describe the building stock of Thessaloniki.

Type	Structural system	Height (number of storeys)	Seismic design level
RC1	Concrete moment frames	(L)ow-rise (1-3) (M)id-rise (4-7) (H)igh-rise (8+)	(N)o/pre code (L)ow code (M)edium code (H)igh code
RC3	Concrete moment frames with unreinforced masonry infill walls		
	RC3.1 Regularly infilled frames		
	RC3.2 Irregularly infilled frames (pilotis)		
RC4	RC dual systems (RC frames and walls)		
	RC4.2 Regularly infilled dual systems		
	RC4.2 Irregularly infilled dual systems (pilotis)		
MBr	Unfeinforced masonry of bricks	12 (1-2)	
		3+ (3 or more)	
MSt	Unfeinforced masonry of stone	12 (1-2)	
		3+ (3 or more)	

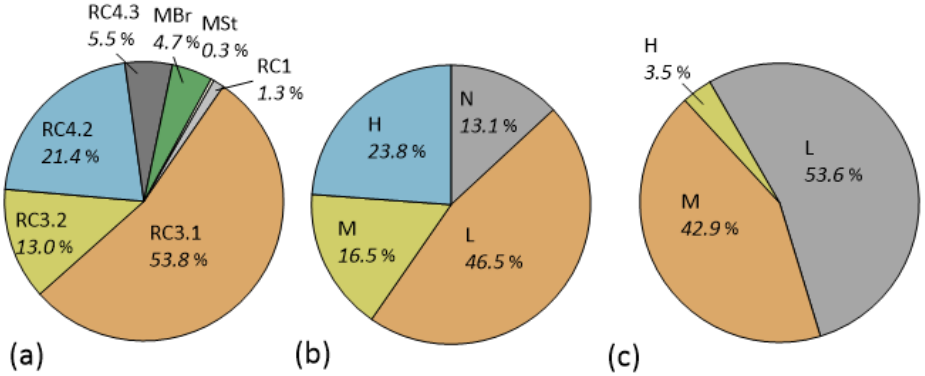

Fig. 8. Classification of the building taxonomies in the study area based on a) material and lateral load resisting system (LLRS), b) code level and c) height category according to the Kappos et al. (2006) taxonomy scheme of **Table 2**.

4 Vulnerability

Fragility models are a critical component of any seismic risk assessment methodology as they describe the probability of exceeding a damage state conditional to a ground shaking intensity (Silva et al., 2019). They may be developed from analyses of appropriate mechanical models, statistical analysis of damage data, expert judgment or with a combination of the above-mentioned approaches (Kappos et al., 2006). Vulnerability

models, i.e., the probability of loss ratio conditional on a set of ground shaking intensities can be produced by the fragility functions using a damage-to-loss model, which expresses the relation between a damage state and the corresponding fraction of loss.

For large scale seismic risk analyses, e.g., at urban, national, continental or even global scale, generic fragility and vulnerability models are usually applied, covering the most common building typologies, such as the model by Martins and Silva (2021), which has been applied at the global seismic risk model developed by of the Global Earthquake Model (GEM) Foundation. These generic models are inevitably developed mainly analytically due to the lack of sufficient empirical damage data to cover all possible building typologies and all seismic intensities in different regions of the world (e.g., Martins and Silva 2021; Romão et al., 2021). For simplicity reasons, their development is usually based on analyses of equivalent single-degree-of-freedom (SDOF) oscillators. Generic models may also be obtained with the combination of analytical methodologies and empirical data, such as the models by Kappos et al. (2006; 2010), which have been derived from analyses of 2D numerical models, representative again for specific building typologies, combined with statistical data from past earthquakes. Finally, for cases of buildings with strategic interest, such as hospitals or schools, building-specific fragility functions can be developed from nonlinear analysis of detailed 3D numerical models, which may be updated through field measurements (Karapetrou et al., 2016; Fotopoulou et al., 2022).

The selection of the fragility / vulnerability model is one of the most significant sources of uncertainties in seismic risk assessment (Riga et al., 2017), as the dispersion observed between fragility functions available in the literature for similar building typologies can be very high (Silva et al., 2019). In the present study we investigate the effect of the selection of fragility and vulnerability models by applying a) the ESRM20 fragility and vulnerability models (Romão et al., 2021) in combination with the GED4ALL exposure and b) the Kappos et al. (2006; 2010) fragility and vulnerability models, in combination with the Kappos et al. (2006) exposure model.

The ESRM20 models have been derived for simplified equivalent single degree-of-freedom oscillators and their use is recommended for large scale applications (e.g., the European building stock). These functions use as intensity measures PGA and spectral accelerations, S_a(0.3s), S_a(0.6s) and S_a(1.0s) depending on building typology. More specifically, for each building typology the final intensity measure is selected as that with the lowest lognormal dispersion in the fragility function, given that it is related to efficiency (Crowley et al., 2021). Following this approach, for the building typologies in the exposure model of Thessaloniki (Section 3.1), S_a(1.0s) is the most commonly adopted intensity measure, as is shown in Fig. 9. Probabilities of exceedance are provided for four damage states, i.e., slight, moderate, extensive and complete, with the thresholds between the different damage states expressed in terms of yield and ultimate displacement in the capacity curves.

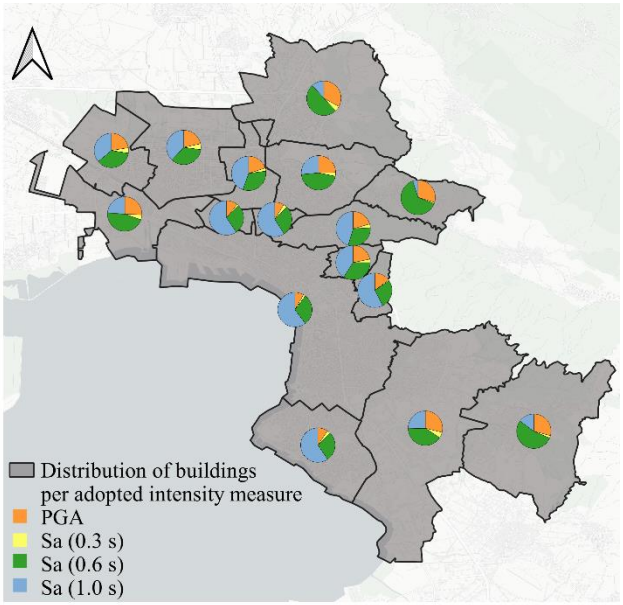

Fig. 9. Distribution of the residential buildings in the exposure model of Thessaloniki per adopted intensity measure in the Romão et al. (2021) vulnerability models

The Kappos et al. (2006; 2010) are based on a hybrid approach, which is a combination of statistical data with appropriately processed results from inelastic analyses of advances 2D numerical models. However, in this application we used only the analytical component of the fragility models (G. Panagopoulos, personal communication), as the hybrid functions are not available for all building types in the exposure model. Fragility functions by Kappos et al. (2006; 2010) use PGA as an intensity measure for all building types, a selection which has often been questioned for flexible buildings. Probabilities of exceedance are provided for five damage states, DS1 (slight), DS2 (moderate), DS3 (substantial to heavy), DS4 (very heavy) and DS5 (collapse), with the thresholds between the different damage states expressed in terms of loss indices for RC structures and in terms of yield and ultimate displacement for masonry structures.

We should highlight that there is no direct compatibility between the damage states which share the same damage state label (e.g. slight, moderate etc) in the two above-mentioned vulnerability models, as the definition of the damage states is not the same. However, we can try to make a rough correspondence between the damage states of the two models by comparing the values of the loss indices (ratio of repair cost to replacement cost) used to relate the distribution of physical damages to the probability of damage repair cost (Table 3). Based on Table 3, slight, moderate, extensive and complete damage in ESRM20 can be roughly matched to DS2, DS3, DS4 and DS5 damage states by Kappos et al. (2004;2010) respectively. This correspondence will be used in the following to compare the damages estimated with the two fragility models.

Table 3. Damage states and loss indices for the ESRM20 and Kappos et al. (2006;2010) vulnerability models

ESRM20		Kappos et al. (2006;2010)		
Damage state	Loss index	Damage state	Range of loss index	Central loss index
		DS1	0.005	0.005
slight	0.05	DS2	0.05	0.05
moderate	0.15	DS3	0.2	0.2
extensive	0.6	DS4	0.45	0.45
Complete	1.0	DS5	0.80	0.80

The fragility curves of the two models cannot be directly compared due to the differences in (a) the way the building classes are defined in the two taxonomy schemes, (b) the adopted intensity measures, (c) the definition of the damage states. Their performance will be compared through the comparison of the estimated damages and mainly, economic losses in the study area. However, indicative fragility and vulnerability curves of the two models for the most common building typologies in the exposure model with the GED4ALL and the Kappos et al. (2006) taxonomies are plotted in Fig. 10 and Fig. 11 respectively.

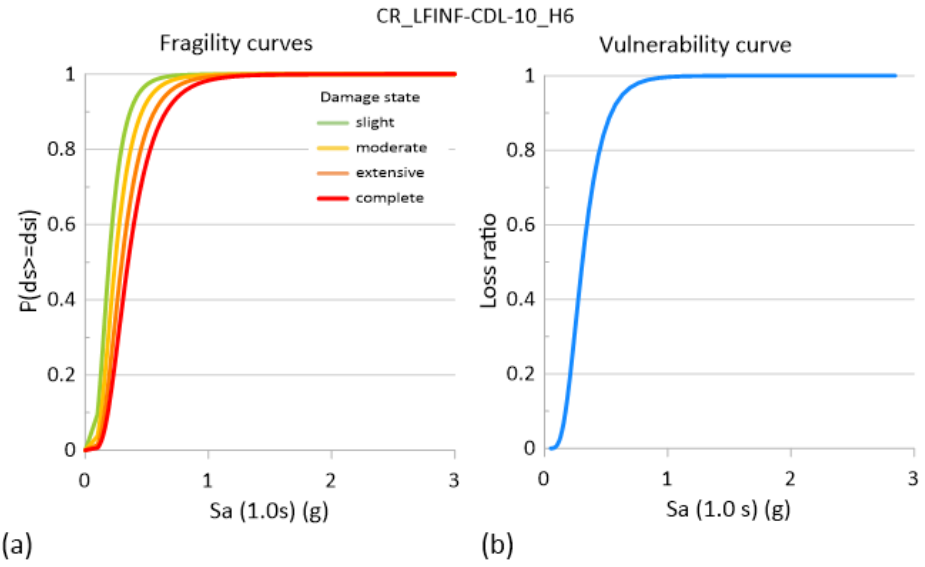

Fig. 10. Indicative fragility curves (a) and vulnerability curve (b) for the most common building typology in Thessaloniki for the exposure model with the GED4ALL taxonomy, i.e., reinforced concrete (CR) - infilled frame (LFINF) - low ductility (CDL-10) - 6 storey (H6) buildings.

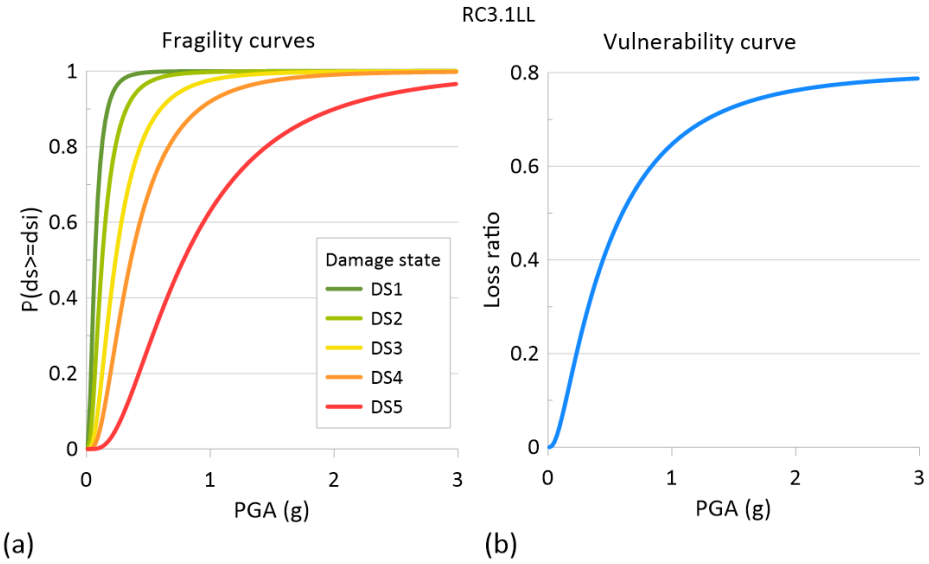

Fig. 11. Indicative fragility curves (a) and vulnerability curve (b) for the most common building typology in Thessaloniki for the exposure model with the Kappos et al. (2006) taxonomy, i.e., reinforced concrete - infilled frame (RC3.1) – low height (L) – low ductility (L).

5 Physical damages

Expected physical damages have been derived through scenario-based damage analyses with precomputed ground motion fields in OpenQuake Engine (Pagani et al., 2014; Silva et al., 2014) where the seismic hazard estimated with Approach 1 and 2 (Section 2) and the exposure models with the GED4ALL and the Kappos et al. (2006) taxonomies (Section 3) and the respective fragility models (Section 4) are combined to estimate the probabilities of exceedance for all the damage states, resulting in a total number of four analyses.

Fig. 12 shows the distribution of the aggregate damage for the whole study area for the two fragility models (ESRM20 and Kappos et al. 2006;2010) combined with the two hazard cases (Approach 1 and Approach 2). To examine the effect of the selection of the fragility model, expected damages estimated with the same site modelling approach (1 or 2) and with different fragility models are compared. In this regard, as mentioned in the previous section, the two fragility models differ on the definition of the damage states, however a rough correspondence between the two models based on the loss indices can be the following: slight, moderate, extensive and complete damage in ESRM20 can be matched to DS2, DS3, DS4 and DS5 damage states by Kappos et al. (2006; 2010) respectively (Table 3). Based on this assumption, 80-85% of the buildings in the study area are estimated to show no or slight damage using the ESRM20 fragility model depending on site modelling approach, while using the Kappos et al. (2006;2010) model this percentage is approximately 50% (DS0+DS1+DS2). Also, according to ESRM20, around 5% of the total number of buildings, i.e., 3,730 buildings, are

expected to collapse, while using the Kappos et al. (2006;2010) model these numbers are doubled, thus leading to more devastating scenarios of about 10-11 % of the buildings to be expected to collapse. At this point we should highlight that in this application we used the purely analytical functions by Kappos et al. (2006; 2010), which often tend to overestimate damages due to some conservative assumptions used in the modelling of the structures. The use of the hybrid functions would probably lead to less severe damages, but this would require adequate damage data from past events for a lot of typologies and for different intensities. In any case, given the uncertainties involved in the development of the different fragility models, the discrepancies between the two models may be considered to be within reasonable limits.

Regarding the site modelling method, this does not seem to significantly affect the distribution of the aggregate damage for the whole study area. This, however, may not be the case when moving to smaller-scale level of analysis, as shown in Riga et al. (2022).

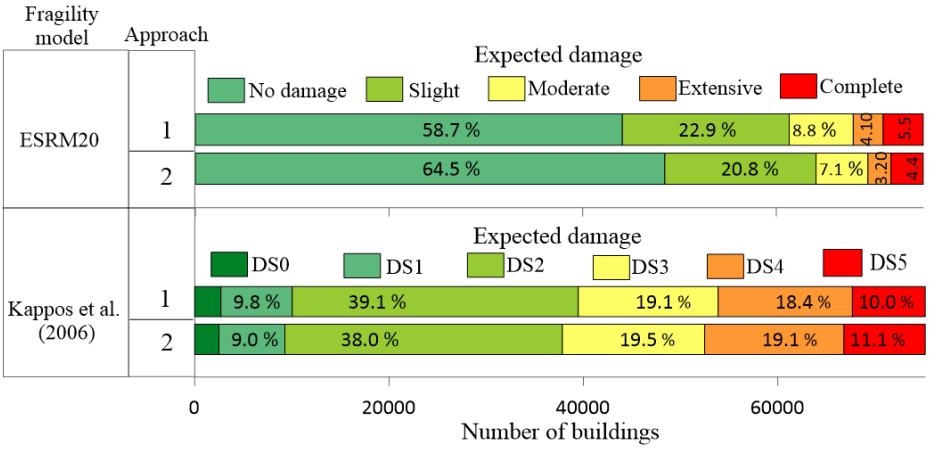

Fig. 12. Aggregate damage distribution of the residential buildings of Thessaloniki, using the fragility model by Romão et al. (2021) and the fragility model by Kappos et al. (2006; 2010) for a seismic hazard with a 475-year return period, estimated using Approach 1 (detailed site model) and Approach 2 (Pitilakis et al., 2020).

Indeed, when moving to municipality level the effect of site modelling method in the estimated seismic damage is becoming more obvious (Fig. 13). For instance, using the ESRM20 fragility model there are significant discrepancies at the south-east coastal area (Kalamaria region, see Fig. 1), where Approach 2 with the amplification factors by Pitilakis et al. (2020) results in significantly higher percentage of complete damage (15.5%, Fig. 13b) compared to Approach 1 with the detailed site model (7.5%, Fig. 13a). This is justified by the increased hazard values in terms of S_a(1.0s) (Fig. 6) in this area with Approach 2, due to the high amplification values for S_a(1.0s) in soil types C3 and D. It is reminded that S_a(1.0s) is used as intensity measure by the ESRM20 fragility model for the majority of the buildings in the area (Fig. 9). On the contrary, for the fragility model by Kappos et al. (2006; 2010), this percentage is higher for Approach 1

(12%, Fig. 13c) compared to Approach 2 (9%, Fig. 13d), as the only intensity measure used in this model, i.e. PGA, is higher for Approach 1 in Kalamaria (Fig. 5). However, the overall discrepancies of the two site modelling methods are smoothed down in this case, making the simplified Approach 2 equally efficient with the more demanding Approach 1. Regarding the effect of the adopted fragility model, the Kappos et al. (2006;2010) model leads to significantly higher percentages of extensive and complete damages of the buildings in all municipalities compared to the ESRM20 fragility model, as was the case for the whole study area.

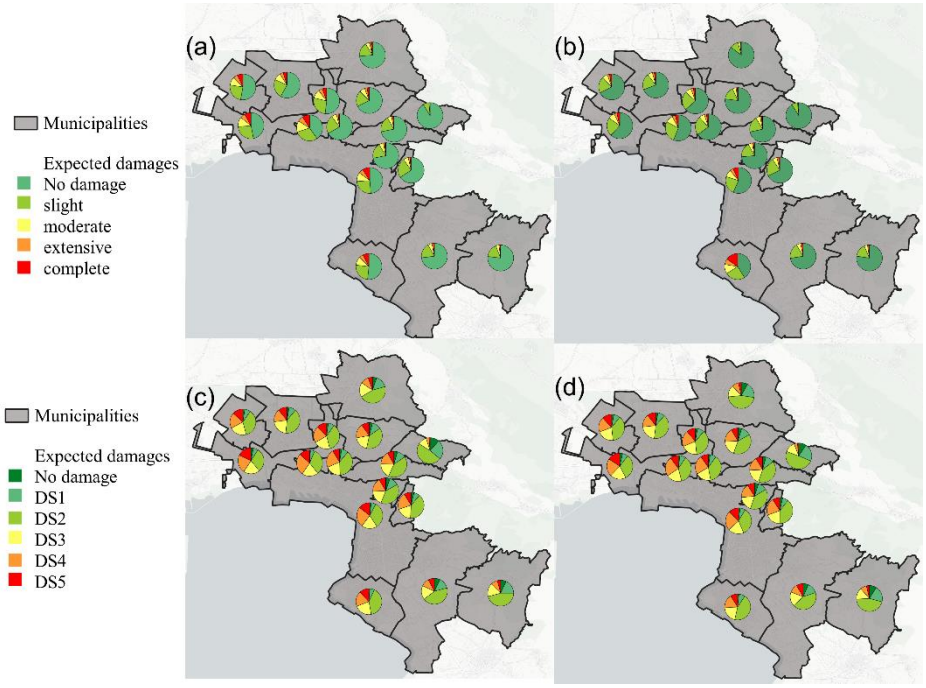

Fig. 13. Spatial distribution of the expected damages of the residential buildings of Thessaloniki using (a) the Romão et al. (2021) fragility model and Approach 1, (b) the Romão et al. (2021) fragility model and Approach 2, (c) the Kappos et al. (2006; 2010) fragility model and Approach 1 and (d) the Kappos et al. (2006;2010) fragility model and Approach 2.

Similar observations can be made when moving to even smaller scale, as is shown in Fig. 14, which illustrates the percentages of the buildings which are expected to be in the complete (for ESRM20) / DS5 (for Kappos et al. 2006; 2010) damage state at census sector level. It is reminded that all census sectors have more or less the same number of residences. This damage state was selected due to its devastating nature and to its comparability in the two fragility models. Using the ESRM20 fragility model, the effect of the site modelling at the Kalamaria region discussed above is confirmed (Fig. 14a and Fig. 14b). In addition, the results for the municipality of Thessaloniki (see Fig. 1), i.e., the center of the broader metropolitan area, are of great interest. The municipality

of Thessaloniki has a total of 20,680 residential buildings, representing 27.5 % of the residential buildings of the whole study area. 74.5% of the buildings in the municipality of Thessaloniki are designed with low code level or even no seismic code at all. The results of the seismic risk analyses show higher percentages of complete damage in the coastal area than in the rest of the municipality in all four analyses (Fig. 14). The highest percentages are observed in the southern part of the coastal area for the case of ESRM20 fragility model and Approach 2 (around 40%), where the soft soil D and the accompanying amplification factors of Pitilakis et al. (2020) result in higher S_a(1.0s) values (see Fig. 6b) and, thus, in higher damages than Approach 1. The Kappos et al. (2006; 2010) fragility model adopts the PGA values which are higher in this area compared to the rest of the municipality, especially with site modelling Approach 1, leading to a significant percentage of buildings in DS5, around 20-30%. We should note, however, that the sectors in the coastal area, despite their large area in some cases, have more or less the same number of buildings as the rest of the sectors in the municipality, and thus do not affect significantly the aggregate probability of complete damage for the whole municipality, which comes up to 16% (see Fig. 13c and Fig. 13d). On the contrary, the municipality of Pefka (see Fig. 1) shows the lowest seismic risk in terms of structural damage. The comparatively new building stock (71.3 % of the buildings were constructed after 1996, thus designed with high code level) in combination with the relatively low seismic hazard in the area lead to small probabilities of complete or extensive damages for all analyses.

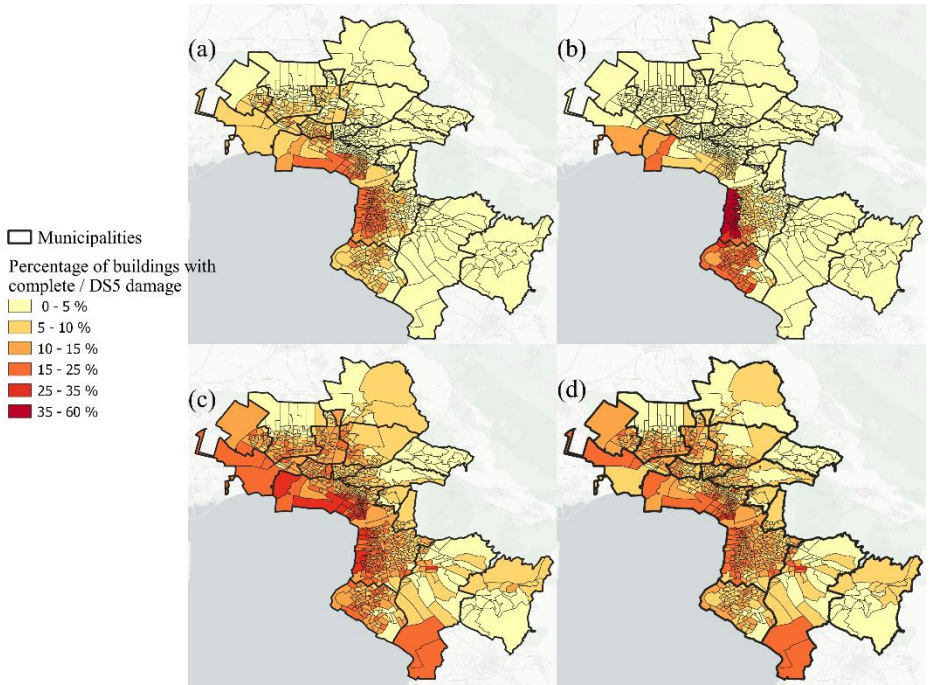

Fig. 14. Spatial distribution of the percentage of the residential buildings with complete damage using (a) the Romão et al. (2021) fragility model and Approach 1 (b) the Romão et al. (2021) fragility model and Approach 2, (c) the Kappos et al. (2006; 2010) fragility model and Approach 1 and (d) the Kappos et al. (2006; 2010) fragility model and Approach 2.

6 Economic losses

Expected economic losses have been derived through scenario-based risk analyses with precomputed ground motion fields in OpenQuake Engine (Pagani et al., 2014; Silva et al., 2014) where the seismic hazard estimated with Approach 1 and 2 (Section 2) and the exposure models with the GED4ALL and the Kappos et al. (2006) taxonomies (Section 3) and the respective fragility models (Section 4) are combined to estimate the economic losses and loss ratios, resulting in a total number of four analyses. For all analyses we assumed a replacement cost of 1000 €/m^2, which is the average cost proposed by ESRM20 for the study area.

The aggregate economic losses for the study area, as well as the total loss ratio, estimated as the ratio between the total replacement cost and the total repair cost, resulting from the four analyses are included in Table 4, while Fig. 15 illustrates the spatial distribution of loss ratio at the study area at census sector level.

Table 4. Expected aggregate economic losses and loss ratios for the residential buildings of Thessaloniki for seismic hazard with a 475-year return period

Vulnerability model	Seismic hazard	Aggregate economic losses	Aggregate Loss ratio
ESRM20	Approach 1 - Detailed site model	4.4 billion €	0.12
	Approach 2 - Pitilakis et al. (2020)	3.8 billion €	0.11
Kappos et al. (2006;2010)	Approach 1 - Detailed site model	8.8 billion €	0.25
	Approach 2 - Pitilakis et al. (2020)	8.2 billion €	0.24

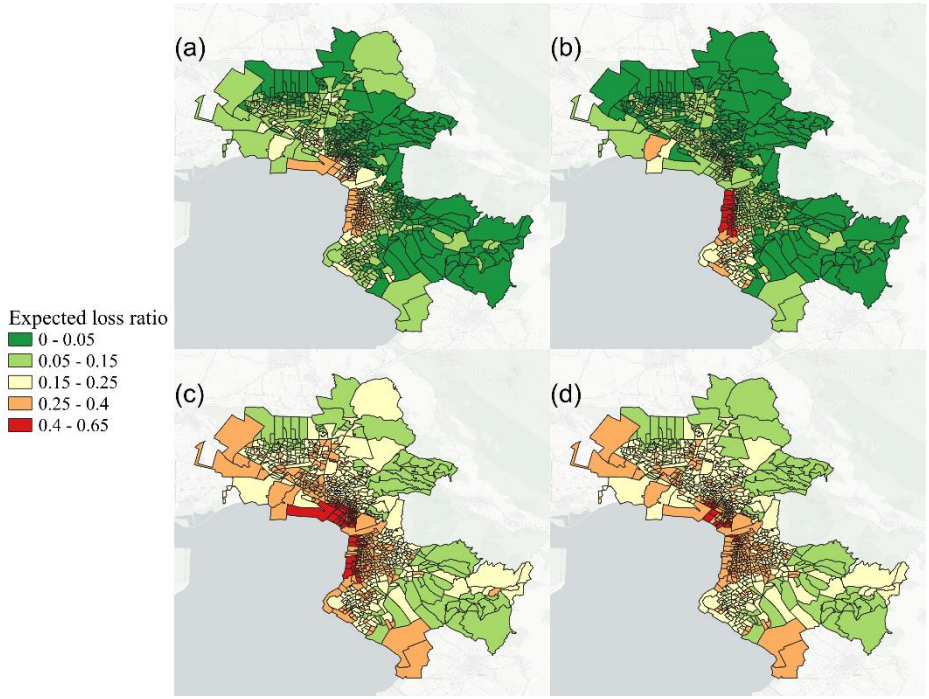

Fig. 15. Spatial distribution of the expected loss ratio of the residential buildings of Thessaloniki using (a) the Romão et al. (2021) fragility model and Approach 1, (b) the Romão et al. (2021) fragility model and Approach 2, (c) the Kappos et al. (2006) fragility model and Approach 1 and (d) the Kappos et al. (2006) fragility model and Approach 2

It is obvious that the Kappos et al. (2006; 2010) vulnerability model leads to increased, almost double, aggregate losses compared to ESRM20. Similarly to what was observed for the aggregate damages, the site modelling method does not affect the aggregate economic losses and the aggregate loss ratio. However, significant discrepancies, show up when moving to census sector level (Fig. 15). For instance, in the southern part of the coastal area of the municipality of Thessaloniki (see Fig. 1) which has relatively old building stock, the ESRM20 vulnerability model leads to substantially increased loss ratio than the rest of the area, around 30% using Approach 1 and around 45% using Approach 2 (Fig. 15a and Fig. 15b). This is in line with the spatial distribution of $S_a(1.0s)$ values shown in Fig. 6, which is the main intensity measure adopted by ESRM20 for the buildings of this area. On the contrary, using the Kappos et al. (2006) vulnerability model, the estimated loss ratio ranges between 35% and 45% (Fig. 15c and Fig. 15d) with higher values observed in the case of the Approach 1, due to higher PGA values than the ones resulting from Approach 2 in this area. In the municipality of Pefka, which is characterized by lower seismic hazard, the seismic risk in terms of loss ratio is lower than for the rest of the study area. However, even in this case, the vulnerability model by Kappos et al. (2006;2010) leads to slightly higher loss ratio (5-15%) than ESRM20 (less than 5%).

These results are in accordance with the probabilities of complete damage / DS5 shown in Fig. 14. It is reminded that in both vulnerability models, the complete damage / DS5 is mainly affecting the economic losses, as it is the damage state with the highest loss index (ratio of repair cost to replacement cost).

Discussion

The large number of uncertainties involved in the methodological chain of seismic risk assessment (Riga et al., 2017) inevitably makes the ability of a seismic risk model to accurately predict future losses a real challenge. In this work we investigated the effect of two of the most important sources of uncertainties, i.e., the level of precision of the site modelling method and the selection of the fragility and vulnerability models, on the seismic risk assessment of the residential buildings of Thessaloniki, the second largest city of Greece. In this regard, we considered two different approaches for site effects modelling and two different vulnerability models, including in both cases the respective components of the recent European Seismic Hazard (ESHM20, Danciu et al., 2021) and Risk (ESRM20, Crowley et al. 2021) Models, which are expected to be applied widely for large scale seismic risk application in Europe in the near future.

Regarding site modelling for seismic hazard assessment, in Approach 1 we used a detailed $V_{s,30}$ model for the study area based on the microzonation study of Thessaloniki as input in the ESHM20 hazard logic tree, while in Approach 2 we classified the study area into different site classes based on the classification scheme by Pitilakis et al. (2020) and amplifies the ESHM20 hazard for rock using the Pitilakis et al. (2020) amplification factors. Approach 1 is considered as more rigorous compared to Approach 2 which is more simplified. The site modelling certainly affects the seismic hazard output, with Approach 1 resulting in significantly higher PGA values for a return period of 475 years at the coastal area compared to Approach 2. On the contrary, the high amplification factors for S_a(1.0s) by Pitilakis et al. (2020) for the soil types in the coastal area of the centre of Thessaloniki and in Kalamaria, result in an overestimation of S_a(1.0s) with respect to Approach 1. These discrepancies are expected to be propagated in the estimated damages and losses, depending of course on the intensity measures used in the adopted vulnerability models. Indeed, at small scale, i.e., census sector level, significant differences in the estimated damages and losses were observed in these particular areas, with contradictory trends for the two different vulnerability models, due to the different adopted intensity measures. With the ESRM20 vulnerability model, the higher S_a(1.0s) values with Approach 2 result in increased risk in the coastal area and Kalamaria, while with the Kappos et al. (2006; 2010) vulnerability model, the higher PGA values of Approach 1 result in higher risk. However, the observed discrepancies are smoothed down when moving to larger scale, encouraging the use of simplified methods for site modelling at large scale seismic risk analyses at regions lacking detailed information on site parameters. These results are in accordance with the observations made by Riga et al. (2022).

Regarding the effect of the selection of fragility / vulnerability model, this parameter was found to have a much more significant impact on the estimated risk, both at small

scale and large scale. With the models by Kappos et al. (2006; 2010), the estimated number of buildings in DS5 (collapse), as well as the estimated economic losses for the whole study area, are twice the number of the respective estimated with the ESRM20 models regardless of adopted site modelling method. These discrepancies are important, but yet within reasonable limits, considering the very high dispersion observed between fragility functions in the literature for similar building typologies. Part of the discrepancies could be attributed to the differences in the definition of the building typologies and damage thresholds, the adopted intensity measures and the way the functions have been developed, while they are also influenced by the hazard and site effect model adopted in the analysis and the evaluation of the IM. The use of the hybrid functions by Kappos et al. (2006; 2010) instead of the analytical ones adopted in this study would probably lead to less severe damages, but this would require adequate damage data from past events for a lot of typologies and for different intensities.

In overall, the main conclusions with respect to physical damages can be summarized as follows: (a) the highest probabilities of complete damage / DS5 are observed in the central part of the study area, and specifically at the coastal area of the historical center of the town, (b) the Kappos et al. (2006;2010) fragility model overestimates the expected damages compared to ESRM20 (Romão et al., 2021), (c) the site modelling method may affect significantly the results at smaller scale analysis, but at large scale more simplified methods, such as Approach 2, seem to be able to provide reliable results, (d) the fragility models and the intensity measure adopted by the vulnerability model has a significant impact on the results. The same observations can be made for the expected economic losses and loss ratios.

Finally, it is noted that in this study we used only the seismic hazard with a 475-year return period (10% probability of exceedance in 50 years), which is widely adopted by seismic codes for the seismic design of structures. Considering lower or higher return periods, as is often the case for seismic risk analyses, or probabilistic seismic risk assessment may lead to different conclusions.

Acknowledgements

We are grateful to Dr. Georgios Panagopoulos and Professor Andreas Kappos for providing data on the fragility and vulnerability curves by Kappos et al. (2006; 2010), Laurentiu Danciu for his support on ESHM20 and Helen Crowley for her support on ESRM20.

Data and resources

OpenQuake Engine is available for download at https://www.globalquakemodel.org/oq-get-started.
The main datasets and OpenQuake input files of ESHM20 and ESRM20 are online available at https://gitlab.seismo.ethz.ch/efehr.
The results of the ESHM20 are open to access and download at hazard.efehr.org, whereas those of the ESRM20 are distributed by risk.efehr.org.

References

Anastasiadis, A., Raptakis, D., Pitilakis, K.: Thessaloniki's detailed microzoning: subsurface structure as basis for site response analysis. Pure and Applied Geophysics, 158 (12), 2597–2633 (2001).

Brzev, S., Silva, V., Allen, L., Scawthorn, C., Yepes, C., Dabbeek, J., Crowley, H.: A building classification scheme for multi-hazard risk assessment. Submitted to Natural Hazards and Earthquake System Sciences (2021).

Crowley, H., Dabbeek J., Despotaki, V., Rodrigues, D., Martins, L., Silv,a V., Romão, X., Pereira, N., Weatherill, G., Danciu, L. : European Seismic Risk Model (ESRM20). EFEHR Technical Report 002 V1.0.0, https://doi.org/10.7414/EUC-EFEHR-TR002-ESRM20 (2021).

Danciu, L., Nandan, S., Reyes, C., Basili, R., Weatherill, G., Beauval, C., Rovida, A., Vilanova, S., Sesetyan, K., Bard, P-Y., Cotton, F., Wiemer, S., Giardini, D.: The 2020 update of the European Seismic Hazard Model: Model Overview. EFEHR Technical Report 001, v1.0.0, https://doi.org/10.12686/a15 (2021).

ELSTAT (2011): 2011 Population-Housing Census, Hellenic Statistical Authority

Fotopoulou, S., Karafagka, S., Petridis, C., Manakou, M., Riga, E., Pitilakis, K.: Vulnerability assessment of school buildings: Generic versus building-specific fragility curves (in preparation) (2022).

Kappos, A., Panagopoulos, G., Panagiotopoulos, C., Penelis, G.: A hybrid method for the vulnerability assessment of R/C and URM buildings. Bulletin of Earthquake Engineering, 4(4), 391–413. https://doi.org/10.1007/s10518-006-9023-0 (2006).

Kappos, A. J., Panagopoulos, G. Fragility curves for reinforced concrete buildings in Greece. Structure and Infrastructure Engineering, 6(1–2), 39–53. (2010).

Kotha, S.R., Weatherill, G., Bindi, D., Cotton, F.: A regionally-adaptable ground-motion model for shallow crustal earthquakes in Europe. Bulletin of Earthquake Engineering 18, 4091–4125 (2020).

Martins, L., Silva, V.: Development of a Fragility and Vulnerability Model for Global Seismic Risk Analyses, Bulletin of Earthquake Engineering 19, 6719–6745 (2021).

Pagani, M., Monelli, D., Weatherill, G., Danciu, L., Crowley, H., Silva, V., Henshaw, P., Butler, L., Nastasi, M., Panzeri, L., Simionato, M., Vigano, D.: OpenQuake Engine: An open hazard (and risk) software for the Global Earthquake Model, Seismological Research Letters, 85 (3), 692-702 (2014).

Pitilakis, K., Riga, E., Anastasiadis, A.: Towards the revision of EC8: Proposal for an alternative site classification scheme and associated intensity-dependent amplification factors. In 17th World Conference on Earthquake Engineering, Sendai, Japan (2020).

Riga, E., Karatzetzou, A., Mara, A., Pitilakis, K: Studying the uncertainties in the seismic risk assessment at urban scale applying the Capacity Spectrum Method: the case of Thessaloniki. Soil Dynamics and Earthquake Engineering, 92, 9–24 (2017).

Riga, E., Apostolaki, S., Karatzetzou, A., Danciu, L., Pitilakis, K: The role of site modelling in seismic hazard and risk assessment at urban scale. The case of Thessaloniki, Greece. Italian Journal of Geosciences (under review) (2022).

Romão, X., Pereira, N., Castro, J.M., De Maio, F., Crowley, H., Silva, V., Martins, L.: European Building Vulnerability Data Repository. Zenodo. https://doi.org/10.5281/zenodo.4062410 (2021).

Silva, V., Crowley, H., Pagani, M., Monelli, D., Pinho, R.: Development of the OpenQuake engine, the Global Earthquake Model's open-source software for seismic risk assessment. Natural Hazards, 72 (3):1409-1427 (2014).

Silva, V., Akkar, S., Baker, J., Bazzurro, P., Castro, J.M., Crowley, H., Dolsek, M., Galasso, C., Lagomarsino, S., Monteiro, R., Perrone, D., Pitilakis, K., Vamvatsikos, D.: Current challenges and future trends in analytical fragility and vulnerability modeling. Earthquake Spectra 35 (4), 1927-1952 (2019).